

Catalytic Generation of Hydrogen with Titanium Citrate and a Macrocyclic Cobalt Complex

Ewa Szajna-Fuller^[a] and Andreja Bakac^{*[a]}

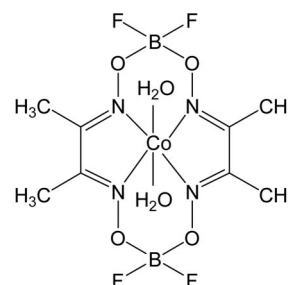
Keywords: Hydrogen / Cobalt / Titanium / Macrocycles / Kinetics / Hydrides

Hydrogen evolution from acidic aqueous solutions of Ti^{III} citrate is strongly catalyzed by $\text{Co}(\text{dmgBF}_2)_2$. The reaction generates an intermediate with maximum absorbance at 770 nm. The slow disappearance of this intermediate takes place simultaneously with the generation of H_2 in a process that was most efficient at pH 1.6 (turnover number 53). The loss of the catalytic activity is caused by the loss of the macrocyclic ligand and formation of $\text{Co}_{\text{aq}}^{2+}$. Control experiments implicate Co^{III} as the most likely oxidation state responsible

for catalyst destruction, and thus provide indirect evidence for the involvement of Co^{III} in the catalytic cycle. Taken together, the data suggest that hydrogen generation takes place at least in part by the $\text{H}^+/\text{HCo}^{\text{III}}(\text{dmgBF}_2)_2$ route. In citrate-containing solutions at $7 \leq \text{pH} \leq 8$, the protonation of $\text{Co}^{\text{I}}(\text{dmgBF}_2)_2^-$ to yield $\text{HCo}^{\text{III}}(\text{dmgBF}_2)_2$ has a rate constant $k_H = 1.4 \times 10^6 \text{ M}^{-1} \text{ s}^{-1}$. This reaction is about ten times slower in the absence of citrate.

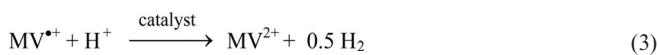
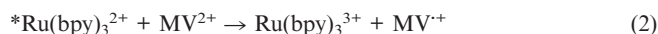
Introduction

In its simplest design, photochemical hydrogen evolution from water requires a photosensitizer (such as polypyridine complexes of ruthenium^[1–4] or iridium^[5]), electron relay (such as methyl viologen, MV^{2+}), and a sacrificial reductant (Red). Frequently used reductants in kinetic and mechanistic studies are triethylamine (TEA), triethanolamine (TEOA), nicotinamide adenine dinucleotide (NADH), and ethylenediamine-*N,N,N',N'*-tetraacetic acid (EDTA). The chemistry involved is shown in Equations (1), (2), and (3) for the $\text{Ru}(\text{bpy})_3^{2+}/\text{MV}^{2+}$ example. The direct reduction of H^+ by MV^+ and other reduced mediators in Equation (3) is slow and requires a catalyst. Colloidal platinum,^[6] $\text{Rh}(\text{bpy})_3^{2+}$,^[1,5] and, more recently, $\text{Co}^{\text{II}}(\text{dmgBF}_2)_2(\text{solvent})_2$ [hereafter $\text{Co}^{\text{II}}(\text{dmgBF}_2)_2$]^[7,8] and derivatives^[2,9] have been explored for this purpose. The diaqua derivative of $\text{Co}(\text{dmgBF}_2)_2$ is shown below.



Among the more efficient photochemical systems that use $\text{Co}^{\text{II}}(\text{dmgBF}_2)_2$ as a catalyst are those based on $[\text{Ir}(\text{ppy})_2(\text{phen})](\text{PF}_6)$ (ppy = 2-phenylpyridine) and $\text{ReBr}(\text{phen})(\text{CO})_3$ (phen = 1,10-phenanthroline) as photosensitizers and $\text{Et}_3\text{N}/\text{Et}_3\text{NH}^+$ buffer as a reductant and proton source in acetone.^[8] Hydrogen yields under visible irradiation exceeded a turnover number of 270 with a turnover frequency of 50 h^{-1} . Quantum yields of 0.10 and 0.16 for the Ir and Re sensitizers, respectively, were reported.^[8] A related cobalt complex, $\text{Co}(\text{dmgH})_2\text{pyCl}$ (dmgH = dimethylglyoxime), is extremely efficient in a system based on a platinum chromophore and TEOA as the sacrificial reductant, producing over 2000 turnovers of H_2 in 10 h in aqueous acetonitrile.^[10]

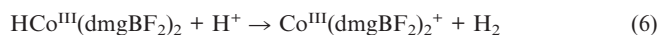
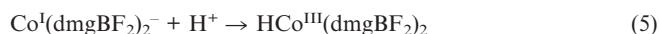
The general mechanism of $\text{Co}^{\text{II}}(\text{dmgBF}_2)_2$ -catalyzed hydrogen ion reduction was elucidated in chemical^[11] and electrochemical^[12,13] studies. In electrochemical experiments, $\text{Co}^{\text{II}}(\text{dmgBF}_2)_2$ is reduced to $\text{Co}^{\text{I}}(\text{dmgBF}_2)_2^-$, followed by the reaction with $\text{H}_2\text{O}/\text{H}^+$ to generate the conjugate acid $\text{HCo}^{\text{III}}(\text{dmgBF}_2)_2$, Equations (4) and (5), respectively. The final step, i.e. H_2 generation, may involve either homolytic or heterolytic cleavage of the $\text{Co}-\text{H}$ bond, as illustrated in Equations (6) and (7).^[11] The importance of the homolytic step, i.e. bimolecular reaction between two hy-



[a] Ames Laboratory, Iowa State University, Ames, IA 50011, USA
Fax: +1-515-294-4709
E-mail: bakac@ameslab.gov

Supporting information for this article is available on the WWW under <http://dx.doi.org/10.1002/ejic.200901176>.

drude molecules, Equation (7), should increase at lower $[H^+]$ where the competing heterolytic $H^+/HCo^{III}(dmgBF_2)_2$ path of Equation (6) will be disfavored. This type of behavior was observed directly in hydrogen evolution studies with a related complex, $HCo(dmghH)_2P(n-C_4H_9)_3$.^[14]



$Co^{II}(dmgBF_2)_2$ -catalyzed reduction of hydrogen ions^[11] by Cr_{aq}^{2+} and Eu_{aq}^{2+} required anions, such as chloride, capable of serving as electron-transfer bridges. The chloride-bridged reduction of $Co^{II}(dmgBF_2)_2$ by Cr_{aq}^{2+} generated a binuclear intermediate $[Cr^{III}-Cl-Co^I(dmgbF_2)_2]^+$ followed by the release of $Co^I(dmgbF_2)_2^-$ and its reaction with H^+ as in Equations (5), (6), and (7). To the extent that reaction (6) was involved, another step was required to close the cycle, namely the reduction of $Co^{III}(dmgbF_2)_2^+$ back to $Co^{II}(dmgBF_2)_2$ by Cr_{aq}^{2+} . H_2 evolution proceeded as long as Cr_{aq}^{2+} was present.^[11]

At this stage of development of various schemes for photocatalytic hydrogen generation, the actual H_2 -forming step from metal hydride appears to be the most critical to address. We have therefore decided to look for reductants for $Co^{II}(dmgBF_2)_2$ that would work well in an integrated photochemical scheme such as that in Equations (1), (2), and (3), at a reasonable pH. The search for both a reductant and buffer has led us to Ti^{III} citrate which is useful in a wide pH range owing to its three carboxyl groups having pK_a s of 3.13, 4.76, and 6.40.^[15] Citrate is also an excellent ligand that binds strongly to a number of metals^[15–17] including titanium.^[18] Owing to its good reducing properties and stability at physiological pH, titanium(III) citrate has found use as a reductant in enzymatic reactions.^[19,20]

The exact chemical composition of Ti^{III} citrate is not known. At pH 4.6, a 2:1 citrate/ Ti^{III} complex was observed^[18] but its structure has not been ascertained. Moreover, the species changes with pH, as evidenced by the changing EPR spectra.^[18] On the basis of the established speciation of titanium(IV) citrate,^[19] and the data suggesting the same number of coordinated citrates in Ti^{III} and Ti^{IV} complexes under comparable conditions,^[18] Ti^{III} citrate in the pH range 3–7 is most likely an equilibrating mixture of bis and tris complexes in various stages of ligand protonation. At pH above 8, mixed hydroxo species are involved, and in strongly acidic solutions (pH 2) a different, unidentified species, perhaps a 1:1 complex, was observed.^[18]

The reduction potential of Ti^{IV}/Ti^{III} citrate (citrate/ Ti^{III} = 2:1) has been reported as -0.48 V vs. NHE.^[21] A much lower value, -0.8 V, was later suggested as more appropriate on the basis of the ability of titanium(III) citrate to reduce bipyridinium salts at pH 8.^[22] Most recently, the potential has been shown to decrease from -0.56 V to -0.63 V as the pH increases from 3 to 6.

The dramatic decrease in the reduction potential for the $Ti^{IV}_{aq}O^{2+}/Ti^{III}_{aq}$ couple ($E^0 = +0.1$ V)^[23] in the presence of citrate makes this combination thermodynamically capable of reducing $Co(dmgbF_2)_2(H_2O)_2$ ($E^0 = -0.43$ V).^[7] Here we have explored the potential of that reaction for hydrogen generation from aqueous solutions.

Results and Discussion

The solubility of $Co(dmgbF_2)_2$ in water is limited, but increases significantly in organic solvents such as ethanol. Solutions of $Co(dmgbF_2)_2$ in both water and mixed water/ethanol solvents are reasonably stable under acidic conditions.^[7] In 5 mM $HClO_4$ at room temperature, about 5% of $Co(dmgbF_2)_2$ (initial concentration 0.1 mM) decomposed in two hours, as determined by a decrease in absorbance at the 456 nm maximum ($\epsilon = 4.06 \times 10^3$ M⁻¹cm⁻¹).^[24] Under the same conditions except that 0.4 M citrate was added, the extent of decomposition in two hours was about 10%.

Solutions of titanium(III) citrate exhibit pH-dependent UV/Vis spectra, Figure 1. The color changes are also visible to the eye, so that solutions containing a 5–6-fold excess of citrate are deep brown at pH > 2.4, but change to purple at pH 1.6 and below. The molar absorptivity of the broad feature at 500 nm increases with increasing pH from 12 M⁻¹cm⁻¹ at pH 0.9 to 35 M⁻¹cm⁻¹ at pH 3.5. The absence of an isosbestic point suggests that multiple species are involved in this transition.

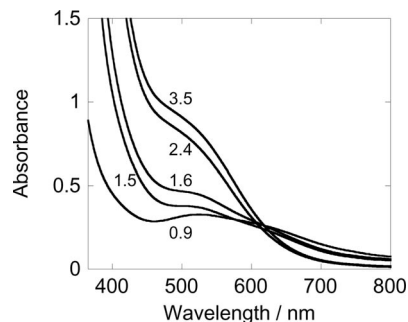


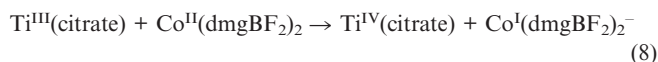
Figure 1. UV/Vis spectra of solutions containing 0.028 M Ti^{III} and 0.77 M citrate at pH 0.9–3.5.

Gas chromatographic (GC) measurements confirmed that H_2 was formed within minutes after the addition of dilute solutions of $Co(dmgbF_2)_2$ to aqueous titanium(III) citrate. To unravel the mechanism and optimize the conditions for hydrogen evolution, we carried out two types of experiments. One set utilized spectrophotometric monitoring of the reactants and of the hydridocobalt intermediate(s), see below, and the other focused on the measurement of H_2 yields. In several cases it was possible to conduct spectroscopic and H_2 -yield measurements under comparable conditions, which made it possible to relate H_2 yields and various experimental parameters. In most cases, however, the two types of experiments required different conditions owing to the need for low absorbance and absence of major quantities of gas in spectrophotometric experiments, but at least moderate amounts of H_2 in GC measurements.

In an effort to learn as much as possible about the species and intermediates involved in hydrogen generation, the kinetic and spectral measurements were carried out in as wide a pH range as possible even though H_2 evolution was observed only at $1 \leq \text{pH} \leq 4$. This approach has allowed us to extrapolate the data and/or observations from higher pH to acidic solutions when direct determinations in the pH regime for H_2 evolution were not possible.

Spectrophotometric Measurements

The mixing of $\text{Co}^{\text{II}}(\text{dmgBF}_2)_2$ with Ti^{III} citrate produced an intensely blue species, λ_{max} 610 nm, characteristic of $\text{Co}^{\text{I}}/\text{HCo}^{\text{III}}$,^[11,25] as in Equations (8) and (5). We expect both forms, Co^{I} and HCo^{III} , to absorb at this wavelength, similar to the closely related $\text{HCo}^{\text{III}}(\text{dmgH})_2\text{P}(n\text{-C}_4\text{H}_9)_3/\text{Co}^{\text{I}}(\text{dmgH})_2\text{P}(n\text{-C}_4\text{H}_9)_3^-$, which has a $\text{p}K_{\text{a}}$ of about 10.5.^[25]



The reduction of $\text{Co}^{\text{II}}(\text{dmgBF}_2)_2$ to $\text{Co}^{\text{I}}(\text{dmgBF}_2)_2^-/\text{HCo}^{\text{III}}(\text{dmgBF}_2)_2$ can be also accomplished with NaBH_4 . As shown in the inset in Figure 2, the spectra generated with Ti^{III} citrate and with NaBH_4 at pH 7.5 are almost identical, supporting our notion that the same species was generated. The somewhat greater intensity of the top spectrum can be accounted for by the presence of excess Ti^{III} citrate which absorbs throughout the visible region, see Figure 1. At pH 7.5, the main form of the reduced cobalt is believed to be $\text{HCo}^{\text{III}}(\text{dmgBF}_2)_2$. Its spectrum (*c* in Figure 2) exhibits λ_{max} 608 nm ($\epsilon_{608} \approx 4.5 \times 10^3 \text{ M}^{-1} \text{ cm}^{-1}$). The related $\text{HCo}^{\text{III}}(\text{dmgH})_2\text{P}(n\text{-C}_4\text{H}_9)_3$ has λ_{max} 610 nm, $\epsilon_{610} \approx 1 \times 10^4 \text{ M}^{-1} \text{ cm}^{-1}$.^[14]

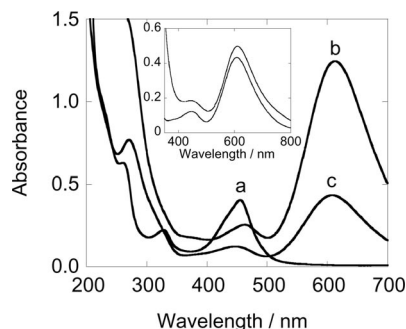


Figure 2. UV/Vis spectra of 0.10 mM $\text{Co}^{\text{II}}(\text{dmgBF}_2)_2$ (a) and of $\text{Co}^{\text{I}}(\text{dmgBF}_2)_2^-/\text{HCo}^{\text{III}}(\text{dmgBF}_2)_2$ prepared from a by reduction with 1.1 equiv. of NaBH_4 at pH 12 (b) and pH 7.5 (c). Inset: UV/Vis spectra of $\text{HCo}^{\text{III}}(\text{dmgBF}_2)_2$ made with 2.6 mM Ti^{III} citrate (top) and 1.1 equiv. of NaBH_4 (bottom) at pH 7.5.

The reduction of $\text{Co}^{\text{II}}(\text{dmgBF}_2)_2$ with NaBH_4 at pH 12 produced a species with λ_{max} 610 nm, $\epsilon_{610} = 1.2 \times 10^4 \text{ M}^{-1} \text{ cm}^{-1}$, which we assign to $\text{Co}^{\text{I}}(\text{dmgBF}_2)_2^-$ (spectrum *b* in Figure 2).

The effect of citrate on the lifetime of $\text{Co}^{\text{I}}(\text{dmgBF}_2)_2^-/\text{HCo}^{\text{III}}(\text{dmgBF}_2)_2$ was examined by reducing $\text{Co}^{\text{II}}(\text{dmgBF}_2)_2$ with stoichiometric amounts of NaBH_4 in the

presence or absence of citrate, and observing the decay of the 610 nm absorbance. In the pH range 7.26–7.80 in the presence of citrate, the absorbance decrease was clearly a two-step process as shown in Figure 3, trace *a*.

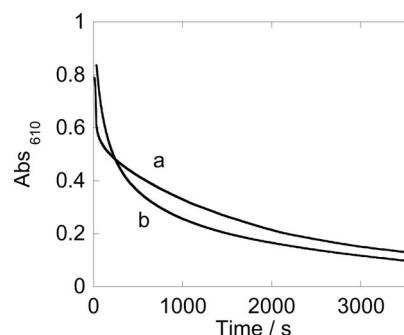


Figure 3. Absorbance decrease at 610 nm. $[\text{Co}^{\text{II}}(\text{dmgBF}_2)_2] = 0.1 \text{ mM}$, $[\text{NaBH}_4] = 0.11 \text{ mM}$, $[\text{citrate}] = 0.4 \text{ M}$ (a) or none (b). Both experiments were performed at pH 7.5.

The kinetics of the fast initial reaction exhibited first-order dependence on $[\text{H}^+]$, as shown in Figure 4, and yielded $k = 1.4 (\pm 0.3) \times 10^6 \text{ M}^{-1} \text{ s}^{-1}$. The observed decrease in absorbance and the rate law are both consistent with this step involving the protonation of $\text{Co}^{\text{I}}(\text{dmgBF}_2)_2^-$ to $\text{HCo}^{\text{III}}(\text{dmgBF}_2)_2$ as in Equation (5). The experimental range of $[\text{H}^+]$ in these experiments was limited by the reaction becoming too fast to measure with our technique at higher $[\text{H}^+]$, and by the inability to lower the $[\text{H}^+]$ reliably past pH 8 with the citrate buffer alone. The use of additional buffers was avoided for fear of further complicating an already complex reaction system.

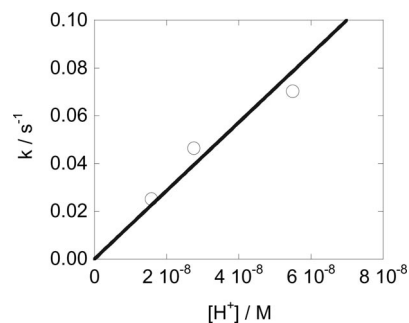


Figure 4. Plot of the rate constant for the reaction of $\text{Co}^{\text{I}}(\text{dmgBF}_2)_2^-$ with H^+ (fast step in trace *a*, Figure 3) against $[\text{H}^+]$. $[\text{Co}^{\text{II}}(\text{dmgBF}_2)_2] = 0.1 \text{ mM}$, $[\text{NaBH}_4] = 0.11 \text{ mM}$, $[\text{citrate}] = 0.4 \text{ M}$.

None the less, the data in Figure 4 and the observation of immeasurably fast kinetics for this step at higher $[\text{H}^+]$ show conclusively that the conversion of redox-generated $\text{Co}^{\text{I}}(\text{dmgBF}_2)_2^-$ to $\text{HCo}^{\text{III}}(\text{dmgBF}_2)_2$ at the pH appropriate for H_2 evolution is fast, i.e. not a kinetic step, on the time scale of the overall reaction. In addition, kinetic data for the protonation of low-valent metal complexes to the corresponding hydrides^[26–28] provide useful insights into the dynamics of metal–hydrogen bonds.

In the absence of added citrate, trace *b* in Figure 3, the data still required a double-exponential fit, but the rate constants for the two stages were now much closer owing to

the faster step in trace *b* being about ten times slower than in trace *a*. The faster formation of $\text{HCo}^{\text{III}}(\text{dmgBF}_2)_2$ in citrate-containing solutions shows that citrate is involved in the reaction either as a proton donor in the protonation step, or as a ligand that made $\text{Co}^{\text{I}}(\text{dmgBF}_2)_2^-$ more susceptible to reaction with H^+ . Qualitatively the same behavior might be expected to persist at pH 1–4 under conditions of H_2 generation as well, although the absolute values of the rate constant k_5 in the presence of citrate is almost certainly different at pH 1–4 than it is at pH 7–8 in view of the changing citrate speciation across the entire pH range examined.

The slow second step in Figure 3 was also acid dependent, but the order in $[\text{H}^+]$ was only about 0.3, Figure 5. The smaller rate constant and a mild $[\text{H}^+]$ dependence allowed us to examine the kinetics of this stage over a much wider pH range, 4–8. Within the error of determination, citrate had no effect.

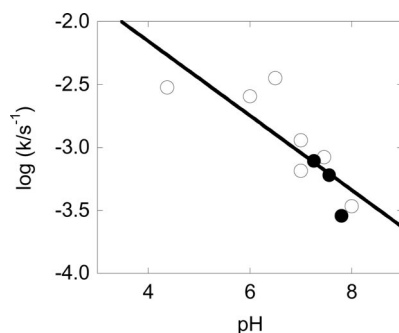


Figure 5. Plot of $\log k$ for the slow step in decomposition of $\text{HCo}^{\text{III}}(\text{dmgBF}_2)_2$ at 610 nm against pH. $[\text{Co}^{\text{II}}(\text{dmgBF}_2)_2] = 0.10 \text{ mM}$, $[\text{NaBH}_4] = 0.11 \text{ mM}$, $[\text{citrate}] = 0.40 \text{ M}$ (filled circles) or zero (open circles).

After the completion of the kinetic runs shown in Figure 5, the UV/Vis spectra revealed that approximately 70% of $\text{Co}^{\text{II}}(\text{dmgBF}_2)_2$ was regenerated in the decay process in the absence of citrate, but only 20% in its presence. Clearly, citrate facilitates the loss of the macrocyclic ligand from cobalt in this pH range.

In the acidic solutions, however, the recovery profile for $\text{Co}^{\text{II}}(\text{dmgBF}_2)_2$ was different. At pH 2.5, the disappearance of $\text{HCo}^{\text{III}}(\text{dmgBF}_2)_2$ was much faster (completed in several hundred seconds), and only about 60% of $\text{Co}^{\text{II}}(\text{dmgBF}_2)_2$ was recovered, but this figure was the same regardless of the presence or absence of citrate. It is unclear whether this result should be attributed to the lower pH or shorter reaction time, but it is obvious that citrate has a minimal effect on the lifetime of $\text{HCo}^{\text{III}}(\text{dmgBF}_2)_2$ under the conditions appropriate for H_2 evolution.

Citrate also affects the stability of $\text{Co}^{\text{III}}(\text{dmgBF}_2)_2^+$, a possible intermediate in the catalytic cycle for the generation of H_2 , Equation (6). A solution of 0.10 mM $\text{Co}^{\text{II}}(\text{dmgBF}_2)_2$ and 0.030 M citrate at pH 2.3 was oxidized with a stoichiometric amount of $\text{Fe}(\text{H}_2\text{O})_6^{3+}$, causing a bleach at 456 nm. To this solution, an equivalent of Ti^{III} citrate was added, which resulted in ca. 80% recovery of the initial 456 nm absorbance. Ion exchange on the column of Dowex

50W-X8 cation exchange resin followed by the thiocyanate/acetone test^[29] revealed that the missing 20% of cobalt was present as $\text{Co}_{\text{aq}}^{2+}$. In a similar experiment in the absence of citrate, and using $\text{Cr}_{\text{aq}}^{2+}$ to reduce $\text{Co}^{\text{III}}(\text{dmgBF}_2)_2^+$, $\approx 95\%$ $\text{Co}^{\text{II}}(\text{dmgBF}_2)_2$ was recovered.^[11] No attempt was made to search for the products of citrate decomposition or oxidation. Such products would be difficult or impossible to detect in the presence of the large excess of citrate used (0.7–1 M) over cobalt (0.1–0.3 mM).

770 nm Intermediate

In acidic solutions containing citrate, the spectrum of $\text{HCo}^{\text{III}}(\text{dmgBF}_2)_2$ exhibits an additional band at 770 nm, Figure 6 and S1 (Supporting Information). At the same time, the intensity of the 610 nm maximum decreases with decreasing pH, and finally disappears at pH 2. Citrate is essential for the 770 nm species regardless of the reductant, Ti^{III} or BH_4^- . The reduction of $\text{Co}^{\text{II}}(\text{dmgBF}_2)_2$ with NaBH_4 in the presence of other anions (acetate, chloride or perchlorate) did not yield the 770 nm band, Figure S2 (Supporting Information).

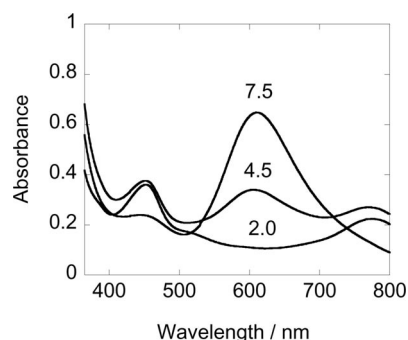


Figure 6. UV/Vis spectra of the reduced cobalt complex obtained from 0.10 mM $\text{Co}^{\text{II}}(\text{dmgBF}_2)_2$ and excess Ti^{III} citrate (2.6 mM Ti^{III} + 0.50 M citrate) at pH 7.5, 4.5, and 2.0.

The 770 nm species most likely has citrate coordinated to hydridocobalt(III) in a monomeric or dimeric arrangement. In the latter case, either citrate or chloride, both of which are present in our solutions, could serve as bridging ligands and facilitate H_2 elimination from two adjacent Co-H sites. As shown later, however, the involvement of a binuclear complex is contradicted by the failure of the system to generate H_2 at $\text{pH} > 4$.

The intermediate absorbing at 770 nm was critical for hydrogen evolution. In fact, the rate of its decay and that of H_2 evolution followed the same time course, as shown by an experiment in Figure 7. Once the absorbance at 770 nm reached a constant minimum value, H_2 evolution also ceased. The addition of more $\text{Co}(\text{dmgBF}_2)_2$ restored both the 770 nm species and hydrogen evolution.

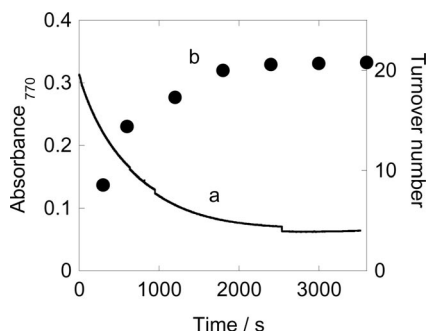


Figure 7. (a) Kinetic trace at 770 nm for solution containing 0.77 M citrate and 0.03 M Ti^{III} and 0.10 mM Co(dmgBF₂)₂ at pH 1.2. (b) The circles represent turnover numbers for H₂ evolution under identical conditions except that [Co(dmgBF₂)₂] = 0.2 mM. The discontinuities in trace *a* were caused by bubble formation.

Hydrogen Evolution

The yields of hydrogen, as determined by gas chromatography, are expressed in Table 1 and Figure 8 as turnover numbers [TON = mol H₂/mol Co(dmgBF₂)₂]. At the end of the experiments shown in Table 1 and Figure 8, all of the catalyst was decomposed and converted to Co(H₂O)₆²⁺.

Table 1. Conditions and turnover numbers for hydrogen production.^[a]

Run	[Co(dmgBF ₂) ₂] [10 ⁻⁴ M]	[Ti ^{III}] [M]	[citrate] _{tot} [M] ^[b]	pH	TON ^[c]
1	2.0	0.12	0.77	1.4	44
2	2.0	0.21	0.67	1.6	50
3	2.0	0.21	0.95	1.6	53
4	2.0	0.21	0.67	1.6	44 ^[d]
5	2.0	0.03	0.77	1.2	21
6	1.0	0.21	0.67	1.6	40
7	3.4	0.21	0.67	1.6	49

[a] Room temperature, aqueous solutions containing 5% ethanol. Total [Cl⁻] = 0.3–0.6 M. [b] Total concentration of citrate. [c] Turnover number = mol H₂/mol Co(dmgBF₂)₂. [d] 0 °C.

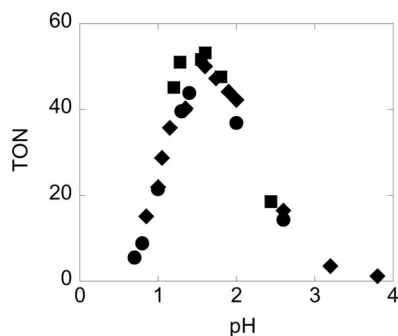


Figure 8. Effect of pH on the turnover number for H₂ generation. Circles: [Ti^{III}] = 0.12 M, [citrate] = 0.77 M; diamonds, [Ti^{III}] = 0.21 M, [citrate] = 0.66 M; squares, [Ti^{III}] = 0.21 M, [citrate] = 0.95 M. All experiments had [Co(dmgBF₂)₂] = 0.2 mM.

Of all the experimental parameters, pH had the greatest effect on hydrogen yields. The highest turnover numbers were obtained at pH 1.4–1.6, with a sharp decline at both higher and lower acidities. The source of the observed dependence is not obvious and is probably a combination of

factors that include the stability of Co(dmgBF₂)₂ (which decreases with increasing [H⁺]), equilibrium constant(s) for cobalt citrate formation (which should increase at higher pH), and the rate of the actual H₂-generating step.

The concentration of reagents other than H⁺ had only a modest effect. An increase in [citrate] from 0.67 M to 0.95 M, increased the H₂ yield by only 6% (Runs 2 and 3). An increase in [Co(dmgBF₂)₂] from 0.1 mM to 0.2 mM yielded ca. 25% more H₂ (Runs 2 and 6), but no further increase was observed at 0.34 mM Co(dmgBF₂)₂ (Run 7). Also, varying Ti^{III} concentration in the range 0.12–0.21 M did not have a noticeable effect, but H₂ yields did decrease significantly at much lower [Ti^{III}] (0.03 M, Run 5). Lowering the temperature to 0 °C caused a small increase in the concentration of the 770 nm species (Figure S3), but H₂ yields were somewhat lower (Run 4). We associate this result with the additional time (one hour) that the solution was allowed to stand at room temperature to equilibrate the gas and solution phases, which probably also caused a greater loss of H₂ gas by diffusion through the septum.

Hydrogen-Forming Step

In view of the reasonable stability of Co^{II}(dmgBF₂)₂ in acidic solutions even in the presence of citrate, we infer that either the Co^I or Co^{III} oxidation state must be responsible for the rapid loss of macrocyclic ligand during the catalytic process. As shown above, both decay readily in acidic solutions, but Co^{III} decay was faster and was accelerated by citrate. HCo^{III}(dmgBF₂)₂ has been shown earlier to be involved in H₂ evolution catalyzed by Cr_{aq}²⁺. In that reaction, the catalyst survived well,^[11] suggesting that HCo^{III}-(dmgBF₂)₂ was sufficiently persistent despite multiple turnovers. The lack of an effect from the citrate on the stability of HCo^{III}(dmgBF₂)₂ at acidic pH (2.5) thus suggests that this species should not be the main reason for catalyst decay in this work. This leaves cobalt(III) as the most probable candidate.

This analysis has implications regarding the mechanism of the H₂-generating step. If Co^{III}(dmgBF₂)₂⁺ (perhaps with a coordinated citrate) is indeed involved, then the most likely source of H₂ is the H⁺/HCo^{III}(dmgBF₂)₂ reaction of Equation (6). Thus, H₂ generation takes place at least in part by heterolytic cleavage of the Co–H bond. The other pathway, Equation (7), may also operate, but we have no direct evidence that would confirm or rule out this possibility. The complete loss of catalytic activity at pH ≥ 4 suggests, however, that the bimolecular path of Equation (7) is either negligibly slow throughout the pH range studied, or that it exhibits an unusual pH dependence and functions only at 0.5 ≤ pH ≤ 4, where it competes with Equation (6). This unlikely scenario cannot be entirely ruled out owing to the changing, but largely unknown speciation of Ti^{III} citrate in the pH range explored.

Conclusions

The reduction of Co(dmgBF₂)₂ with Ti^{III} citrate or with BH₄⁻ generates Co^I(dmgBF₂)₂/HCo^{III}(dmgBF₂)₂ with λ_{max}

at 610 nm at $7.8 \leq \text{pH} \leq 12$. In acidic solutions, but only in the presence of citrate, the absorbance at 610 nm decreased at the expense of a new band at 770 nm. Under such conditions, the solution evolved hydrogen catalytically with a maximum turnover number of 53 at pH 1.5. H_2 evolution was accompanied by the disappearance of the 770 nm species. Moreover, the two processes followed the same time course. When the catalytic activity ceased, all of the catalyst was decomposed and converted to $\text{Co}(\text{H}_2\text{O})_6^{2+}$. The activity could be restored by adding more $\text{Co}(\text{dmgBF}_2)_2$ to the reaction mixture.

The 770 nm species most likely has citrate coordinated to hydridocobalt(III) in a monomeric or dimeric arrangement. Thus, in addition to its role as a ligand for Ti^{III} , citrate seems to be also involved in the hydrogen-generating step, perhaps as an intramolecular proton donor for the hydride. This idea draws some support from the data at higher pH where the protonation of $\text{Co}^{\text{I}}(\text{dmgBF}_2)_2$ to generate $\text{HCo}(\text{dmgBF}_2)_2$ was accelerated by citrate.

The examination of the stability of various cobalt species under the reaction conditions suggests that the loss of the catalyst is a result of the decay of $\text{Co}^{\text{III}}(\text{dmgBF}_2)_2^+$. This result leads us to conclude that H_2 generation takes place at least in part by a heterolytic cleavage of the Co–H bond. Another piece of evidence that supports this mechanism is the lack of hydrogen evolution at $\text{pH} > 4$ where a homolytic, i.e. bimolecular path, should not be greatly disfavored as compared to more acidic solutions.

Experimental Section

General: Solutions of $\text{Ti}^{\text{III}}\text{Cl}_3$, typically 0.5–0.7 M in 0.5 M HCl, were prepared by dissolving titanium sponge in 3 M HCl under argon, filtered, and stored at 0 °C.^[30] Sodium citrate (T. J. Baker), hydrochloric acid and perchloric acid (Aldrich), and piperazine-*N,N'*-bis(4-butanedisulfonic acid) (PIBBS) (GFS Chemicals) were used as received. Solid $\text{Co}(\text{dmgBF}_2)_2$ was prepared as described previously.^[7] Stock solutions (2–4 mM) were prepared in air-free ethanol.

Samples containing Ti^{III} citrate of desired concentrations were prepared by adding appropriate amounts of TiCl_3 (0.01–0.22 M) to aqueous solutions of sodium citrate (0.06–0.95 M). The pH was adjusted with HClO_4 , and the remaining traces of O_2 were removed by purging with argon for 30 min. Air-free ethanolic solution of $\text{Co}^{\text{II}}(\text{dmgBF}_2)_2$ was added to reach the final concentration of the cobalt complex of 0.10–0.34 mM. The samples prepared in this way contained significant amounts of chloride, 0.03–0.66 M. In the absence of citrate, the pH was adjusted with HClO_4 , NaOH, and PIBBS buffer (pK_a 8.55).

Hydrogen production was quantified with gas chromatography. Typically, the sample was shaken vigorously for 30 sec, and 60 μL of the headspace was injected into a GOW-MAC instrument, Series 350 with a thermal conductivity detector equipped with a 5-Å molecular sieve column. Nitrogen was used as a carrier gas. The column temperature was maintained at 70 °C, and the temperature of both injector and detector was 100 °C. The system was calibrated by injecting known amounts of H_2 gas. The pH of the H_2 -generating solutions was measured at the end of each experiment with an Accumet AP71 pH meter.

UV/Vis spectra were obtained with a Shimadzu UV-3101 PC spectrophotometer. The spectra of the unstable acidic solutions of the reduced cobalt complex were run at maximum speed (30 seconds per spectrum in Figures 2 and 3) to minimize losses during the acquisition time. None the less, some decomposition ($\leq 10\%$) of $\text{HCo}(\text{dmgBF}_2)_2$ at the highest acid concentrations could not be avoided. Unless mentioned otherwise, the kinetic data were obtained at 25.0 ± 0.2 °C. Kinetic traces were fitted with Kaleidagraph 4.03 software. In-house distilled water was further purified by passage through a Barnstead EASYpure II system.

Supporting Information (see also the footnote on the first page of this article): Figures S1–S3.

Acknowledgments

This manuscript has been authored with the U. S. Department of Energy under Contract No. DE-AC02-07CH11358.

- [1] S.-F. Chan, M. Chou, C. Creutz, T. Matsubara, N. Sutin, *J. Am. Chem. Soc.* **1981**, *103*, 369–379.
- [2] J. Hawecker, J.-M. Lehn, R. Ziessel, *Nouv. J. Chim.* **1983**, *7*, 271–277.
- [3] J. Kiwi, M. Gratzel, *Nature* **1979**, *281*, 657–658.
- [4] C. V. Krishnan, N. Sutin, *J. Am. Chem. Soc.* **1981**, *103*, 2141–2142.
- [5] E. D. Cline, S. E. Adamson, S. Bernhard, *Inorg. Chem.* **2008**, *47*, 10378–10388.
- [6] J. Kiwi, M. Gratzel, *J. Am. Chem. Soc.* **1979**, *101*, 7214–7217.
- [7] A. Bakac, M. E. Brynildson, J. H. Espenson, *Inorg. Chem.* **1986**, *25*, 4108–4114.
- [8] A. Fihri, V. Artero, A. Pereira, M. Fontecave, *Dalton Trans.* **2008**, 5567–5569.
- [9] P. Du, K. Knowles, R. Eisenberg, *J. Am. Chem. Soc.* **2008**, *130*, 12576–12577.
- [10] P. Du, J. Schneider, G. Luo, W. W. Brennessel, R. Eisenberg, *Inorg. Chem.* **2009**, *48*, 4952–4962.
- [11] P. Connolly, J. H. Espenson, *Inorg. Chem.* **1986**, *25*, 2684–2688.
- [12] C. Baffert, V. Artero, M. Fontecave, *Inorg. Chem.* **2007**, *46*, 1817–1824.
- [13] X. Hu, B. S. Brunschwig, J. C. Peters, *J. Am. Chem. Soc.* **2007**, *129*, 8988–8998.
- [14] T.-H. Chao, J. H. Espenson, *J. Am. Chem. Soc.* **1978**, *100*, 129–133.
- [15] J. P. Glusker, *Acc. Chem. Res.* **1980**, *13*, 345–352.
- [16] M. Matzapetakis, M. Kourgiantakis, M. Dakanali, C. P. Raptopoulou, A. Terzis, A. Lakatos, T. Kiss, I. Banyai, L. Iordanidis, T. Mavromoustakos, A. Salifoglou, *Inorg. Chem.* **2001**, *40*, 1734–1744.
- [17] M. Matzapetakis, C. P. Raptopoulou, A. Tsohos, V. Papaefthymiou, N. Moon, A. Salifoglou, *J. Am. Chem. Soc.* **1998**, *120*, 13266–13267.
- [18] R. Uppal, C. D. Incarvito, K. V. Lakshmi, A. M. Valentine, *Inorg. Chem.* **2006**, *45*, 1795–1804.
- [19] J. M. Collins, R. Uppal, C. D. Incarvito, A. M. Valentine, *Inorg. Chem.* **2005**, *44*, 3431–3440.
- [20] L. C. Seefeldt, S. A. Ensign, *Anal. Biochem.* **1994**, *221*, 379–386.
- [21] A. J. B. Zehnder, K. Wuhrmann, *Science* **1976**, *194*, 1165–1166.
- [22] M. Guo, F. Sulc, M. W. Ribbe, P. J. Farmer, B. K. Burgess, *J. Am. Chem. Soc.* **2002**, *124*, 12100–12101.
- [23] A. J. Bard, R. Parsons, J. Jordan, *Standard Potentials in Aqueous Solution*, Marcel Dekker, New York and Basel, **1985**, p. 540.
- [24] A. Bakac, J. H. Espenson, *J. Am. Chem. Soc.* **1984**, *106*, 5197–5202.

- [25] G. N. Schrauzer, R. J. Holland, *J. Am. Chem. Soc.* **1971**, *93*, 1505–1506.
- [26] E. Fujita, J. F. Wishart, R. van Eldik, *Inorg. Chem.* **2002**, *41*, 1579–1583.
- [27] A. Fortunelli, P. Leoni, L. Marchetti, M. Pasquali, F. Sbrana, S. Massimo, *Inorg. Chem.* **2001**, *40*, 3055–3060.
- [28] J. D. Protasiewicz, K. H. Theopold, *J. Am. Chem. Soc.* **1993**, *115*, 5559–5569.
- [29] R. E. Kitson, *Anal. Chem.* **1950**, *22*, 664–667.
- [30] A. Bakac, M. Orhanovic, *Inorg. Chim. Acta* **1977**, *21*, 173–178.

Received: December 6, 2009
Published Online: May 4, 2010